Insulating band structure of $CuGeO_3$

1999 J. Phys.: Condens. Matter 11 209

(http://iopscience.iop.org/0953-8984/11/1/017)

J. Phys.: Condens. Matter **11** (1999) 209–219. Printed in the UK PII: S0953-8984(99)95951-9

Insulating band structure of $CuGeO_3$

Hua Wu†, Mei-chun Qian† and Qing-qi Zheng†‡

† Institute of Solid State Physics, Academia Sinica, PO Box 1129, 230031 Hefei, People's Republic of China

‡ The State Key Laboratory for Magnetism, Academia Sinica, 100080 Beijing, People's Republic of China

Received 26 June 1998, in final form 23 September 1998

Abstract. The insulating character of the spin–Peierls cuprate $CuGeO_3$ is investigated by adopting a modified linear combination of atomic orbitals (LCAO) band method both within the local spin-density approximation (LSDA) and using the strong-correlation correction (LSDA + U). It is shown that the strongly orbital-dependent exchange splittings of the narrow Cu 3d bands open an insulating gap, and that the strong d–d electron correlations increase the gap substantially. The present results accord with the experimental ones.

1. Introduction

Since the discovery [1] of the first spin–Peierls (SP) inorganic compound, $CuGeO_3$, enormous numbers of experimental and theoretical studies have been carried out [2–9]. Superlattice reflections [2, 3] indicate that the uniform antiferromagnetic (AFM) Cu chains undergo a transformation into a dimerized state at low temperature [10, 11]. The assertion that the ground state is a spin singlet with a finite spin-excitation energy gap, which is responsible for a rapid drop of the magnetic susceptibility to zero below 14 K [1], has been confirmed by an inelastic neutron scattering measurement [12]. In spite of the presence of non-negligible interchain exchange interactions [12], a quasi-one-dimensional (quasi-1D) Heisenberg model gives a reasonable description for the magnetic properties of this material [7–9].

As regards the energy band structure for $CuGeO_3$, a few calculations [13, 14] have been performed, based on the local (spin-) density approximation (L(S)DA). A non-magnetic (NM) metallic state was obtained by using the linearized augmented-plane-wave (LAPW) method [13]. An almost identical result was yielded for both the NM state and the AFM one within the linear muffin-tin orbital method in the atomic sphere approximation (LMTO-ASA) [14]. Additionally, it was shown that a SP distortion can lead to a minor gap, thus stabilizing the SP state to some extent [13, 14]. Unfortunately, the previous calculations did not account well for the insulating character [15] of this strongly correlated cuprate [16, 17].

It is commonly accepted that the L(S)DA usually gives poor descriptions for strongly correlated systems such as transition metal oxides, where on-site Coulomb interactions U of localized d or f electrons could be significant but are generally underestimated by the L(S)DA, a formalism within a weak-coupling mean-field theory [18]. In general, the U-parameter is used on the assumption of a well-defined energy separation between the occupied and the unoccupied states and primarily determines the size of the insulating gap. Produced by making a strong-correlation correction to the L(S)DA, the so-called L(S)DA + U scheme was proposed by Anisimov *et al* [18], and several subsequent modifications [19, 20] were presented. This

0953-8984/99/010209+11$19.50

L(S)DA + U scheme, yielding quite satisfactory results for a few strongly correlated systems, is considered to be a useful approach [18–22].

Recently Šlivenčanin *et al* calculated the band structure for the AFM state of $CuGeO_3$ by using the LMTO-ASA method within the LSDA + U regime [23]. With the d–d electron Coulomb and exchange energy parameters of $U = 9.66$ eV and $J = 0.59$ eV obtained from a constrained density-functional calculation, their calculation gave an insulating gap of 3.02 eV and a spin moment of 0.89 μ_B per Cu ion. As noted in their paper, the considerable value of U may reflect that there is some degree of underscreening, and it was stated in reference [19] that reasonable values of U from the constrained density-functional calculation may still differ by up to 30% between different calculations. A relatively moderate value of $U_{dd} = 6.7$ eV was determined by an electron spectroscopy study [17], which implies that the large gap could be partly due to the overestimated Coulomb repulsions. On the other hand, since no gap is opened for $CuGeO_3$ when U is not turned on [14], one could not apply U unambiguously [24, 25]. For this reason, one would like to obtain a gap (no matter how small) at the level of a density-functional ground-state calculation so as to define the U-correction in an unambiguous fashion [25]. The band calculations have been carried out in this work by adopting a modified LCAO method [26], which is characterized by both a precise treatment of the Hartree potential and an efficient evaluation of multi-centre integrals. As will be seen below, the strongly orbital-dependent exchange splittings due to the anisotropic exchange potential open an insulating gap for this compound, and the strong d–d electron correlations increase the gap substantially and account well for the charge-transfer (CT) insulating character of this cuprate.

In section 2, the modified LCAO band method is described; it is considered to be a full-potential (FP) scheme due to there being no shape approximation for the charge density and crystal potential. In section 3, the results obtained are presented and a discussion is given. Finally, conclusions are drawn in section 4.

2. The computational method

As one of the common band approaches, the LCAO method is typical of methods of solution of the one-electron Schrödinger equation in terms of the crystal potential in using a LCAO set of basis functions in the tight-binding approximation. In practical applications, this equation is generally transformed into a Hohenberg–Kohn–Sham (H–K–S) equation based on the density-functional theory and then solved in the L(S)DA self-consistently. A key point of this method is that of how to evaluate multi-centre integrals efficiently. This problem is solved successfully by means of the partition function scheme [27, 28], as described below.

The first step is to define an atomic partition function [27], $P_i(\vec{r})$, for any atom i with respect to any point $\vec{r}$ in a crystal, and it is required that all $P_i(\vec{r})$ sum to *unity* at any point $\vec{r}$:

$$\sum_i P_i(\vec{r}) = 1. \tag{1}$$

For any given point $\vec{r}_0$ and the neighbouring atoms j of this point, it is feasible to construct a set of $P_j(\vec{r}_0)$ to meet the demand

$$\sum_j P_j(\vec{r}_0) = 1 \tag{2}$$

and for other atoms far away from this point, it is practical to set their partition functions to *zero* over this point. Thus equation (1) is fully satisfied.

By means of an appropriate continuous analogy to the finite-temperature Fermi function of statistical mechanics [27], a set of well-behaved single-centre partition functions are constructed, each of which has a value nearly equal to *unity* near its own nucleus and decreases

smoothly to *zero* far away from the nucleus. Since the construction depends on only the relative atomic positions [27], naturally $P_i(\vec{r})$ possesses the distinct and effective character

$$P_i(\vec{r}) = P_{i'}(\vec{r} + \vec{R}_{i\to i'}) \tag{3}$$

due to the translational symmetry of crystals, where i' refers to the atom achieved by a translation of the atom i by the lattice vector $\vec{R}_{i\to i'}$. For the reason, only a set of $P_i(\vec{r})$ attached to the atoms within a reference unit cell (U.C.) are required to be constructed in practical applications.

Next, the multi-centre integrals are treated within this partition scheme.

An integral over all space for any function $F(\vec{r})$ possessing translational symmetry, e.g., a Hamiltonian and overlapping matrix elements, can be reformulated as follows:

$$\int F(\vec{r})\,\mathrm{d}\vec{r} = \int \sum_i P_i(\vec{r})F(\vec{r})\,\mathrm{d}\vec{r} = \int \left[\sum_k P_k(\vec{r}) + \sum_{k'} P_{k'}(\vec{r})\right] F(\vec{r})\,\mathrm{d}\vec{r} \tag{4}$$

where k and k' denote any atom within the reference U.C. and any one within any other U.C., respectively.

The equation

$$\int P_{k'}(\vec{r})F(\vec{r})\,\mathrm{d}\vec{r} = \int P_k(\vec{r} - \vec{R}_{k\to k'})F(\vec{r} - \vec{R}_{k\to k'})\,\mathrm{d}(\vec{r} - \vec{R}_{k\to k'}) = \int P_k(\vec{r})F(\vec{r})\,\mathrm{d}\vec{r} \tag{5}$$

is derived, according to equation (3). Therefore, one can rewrite equation (4) as follows:

$$\int F(\vec{r})\,\mathrm{d}\vec{r} = N\int \sum_k P_k(\vec{r})F(\vec{r})\,\mathrm{d}\vec{r} = N\sum_k \int F_k(\vec{r})\,\mathrm{d}\vec{r} \tag{6}$$

where N refers to the total number of the unit cells, and the integrand

$$F_k(\vec{r}) = P_k(\vec{r})F(\vec{r}) \tag{7}$$

possesses a single-centre character due to $P_k(\vec{r})$.

Consequently, the multi-centre integral can be evaluated by solving a set of single-centre sub-integrals over a finite space around their respective atoms within only the reference U.C. By using the discrete 3D points in the spherical polar coordinates [27] centred on each nucleus, the multi-centre integral is numerically solved with a high accuracy. For example, an evaluation of the integral for the crystal charge density in NiO gives a value of 287.9395 electron charges for a magnetic U.C. containing eight formula units with 288 electrons. In the same way, a value of the charge equal to 107.9447 electron charges is yielded for a formula unit of $LaCoO_3$ with 108 electrons. The calculational errors are 0.02% and 0.05%, respectively. The error is usually less than 0.2% for more complex systems [26].

A precise potential is required in electronic structure calculations. On the other hand, the partition scheme contributes considerably to an accurate solution for the Hartree potential defined as follows:

$$V(\vec{r}) = \int \frac{\rho(\vec{r'})}{|\vec{r} - \vec{r'}|}\,\mathrm{d}\vec{r'} \tag{8}$$

where the crystal charge density, $\rho(\vec{r})$, is constructed from the following expression:

$$\rho(\vec{r}) = \sum_{\vec{k}} w(\vec{k}) \sum_n^{occ} f_{n\vec{k}} \left|\Psi_{n\vec{k}}(\vec{r})\right|^2 \tag{9}$$

where $w(\vec{k})$ is an integrational weighting of the special $\vec{k}$-points over the irreducible Brillouin zone, and $\Psi_{n\vec{k}}(\vec{r})$ and $f_{n\vec{k}}$ are a single-particle wave function and the corresponding eigenstate occupancy, respectively. $\rho(\vec{r})$ is usually non-spherical in many realistic systems.

One can treat Poisson's equation in the partition scheme instead:

$$\nabla^2 V(\vec{r}) = -4\pi\rho(\vec{r}) = -4\pi \sum_i P_i(\vec{r})\rho(\vec{r}) = -4\pi \sum_i \rho_i(\vec{r}) \tag{10}$$

where the atomic-like charge density, $\rho_i(\vec{r})$, satisfies the equation

$$\rho_i(\vec{r}) = \rho_{i'}(\vec{r} + \vec{R}_{i\to i'}) \tag{11}$$

which is similar to equation (3) due to the translational invariance of $\rho(\vec{r})$.

One can express $V(\vec{r})$ as a sum of individual $V_i(\vec{r})$:

$$V(\vec{r}) = \sum_i V_i(\vec{r}) \tag{12}$$

where $V_i(\vec{r})$ satisfies the single-centre equation

$$\nabla^2 V_i(\vec{r}) = -4\pi\rho_i(\vec{r}). \tag{13}$$

Consequently, the multi-centre Poisson's equation (equation (10)) is reduced to a set of independent single-centre problems (equation (13)), each of which can be numerically solved by spherical harmonic analysis [28] for $\rho_i(\vec{r})$ as follows.

Each $\rho_i(\vec{r})$ is expressed as a spherical harmonic expansion about its own nucleus:

$$\rho_i(r,\theta,\phi) = \sqrt{4\pi} \sum_{\ell m} \sqrt{2\ell+1}\rho_{i\ell m}(r) Y_{\ell m}(\theta,\phi) \tag{14}$$

where the radial function $\rho_{i\ell m}(r)$, called a partial wave of the charge density, is written in the following form:

$$\rho_{i\ell m}(r) = \frac{1}{\sqrt{4\pi}\sqrt{2\ell+1}} \int \rho_i(r,\theta,\phi) Y_{\ell m}(\theta,\phi)\, \mathrm{d}\Omega. \tag{15}$$

The value of $\rho_{i\ell m}(r)$ over each radial point is obtained by performing an angular integration (Ω denotes solid angle) within the angular quadrature approach [29]. Self-consistency of the partial waves is implemented in the present method.

$V_i(\vec{r})$ is also expanded in the same manner as $\rho_i(\vec{r})$:

$$V_i(r,\theta,\phi) = 4\pi\sqrt{4\pi} \sum_{\ell m} \frac{1}{\sqrt{2\ell+1}} V_{i\ell m}(r) Y_{\ell m}(\theta,\phi) \tag{16}$$

and therefore equation (13) is separated into a set of 1D ordinary differential equations:

$$\frac{1}{r}\frac{\mathrm{d}^2}{\mathrm{d}r^2}[r V_{i\ell m}(r)] - \frac{\ell(\ell+1)}{r^2} V_{i\ell m}(r) = -(2\ell+1)\rho_{i\ell m}(r). \tag{17}$$

Each component $V_{i\ell m}(r)$ is calculated by using the Green's function of the Laplacian [28]:

$$V_{i\ell m}(r) = r^{-\ell-1} \int_0^r \rho_{i\ell m}(x) x^{\ell+2}\, \mathrm{d}x + r^{\ell} \int_r^{\infty} \rho_{i\ell m}(x) x^{1-\ell}\, \mathrm{d}x. \tag{18}$$

Finally, the Hartree potential is reconstructed as follows:

$$V(\vec{r}) = 4\pi\sqrt{4\pi} \sum_{i\ell m} \frac{1}{\sqrt{2\ell+1}} V_{i\ell m}(|\vec{r} - \vec{r}_i|) Y_{\ell m}(\theta,\phi). \tag{19}$$

Note that only the single-centre Poisson's equations attached to the atoms within the reference U.C. are required to be solved in practical calculations, according to equation (11). In addition, for the given discrete points used to evaluate the multi-centre integral in equation (6), the summation over atoms i in equation (19) can include just the neighbouring atoms of these points, and the rest, contributed by other atoms far away from these points, can be regarded as a point-charge potential and easily treated by the Ewald summation approach.

As a result, the precise Hartree potential is obtained while maintaining the self-consistency of the partial waves at some finite order ($\ell \leqslant \ell_{max}$). In addition, the exchange–correlation potential can be evaluated by using the self-consistent charge density (expressed by equation (9)) within the L(S)DA formalism. Thus, a possible local anisotropy of both of the potentials would be better manifested, whereas such an anisotropy is almost neglected in a spherical approximation. In this sense, the present method is considered to be a FP scheme due to there being no shape approximation for the charge density and the potentials. Its validity has been verified by a few test calculations. For example, both the resulting gap of 0.3 eV for NiO and a NM ground state for $LaCoO_3$ are consistent with the results obtained within other methods [26].

In spite of the many successes in describing the ground-state properties of various materials, the L(S)DA usually yields poor results for the strongly correlated systems. In this work, the LSDA + U calculation is also performed in order to confirm the insulating character of $CuGeO_3$. The one-electron potential

$$V_{m\sigma}^{\mathrm{LSDA}+U} = V^{\mathrm{LSDA}} + U\sum_{m'}(n_{m'-\sigma} - n^0) + U\sum_{m'(\neq m)}(n_{m'\sigma} - n^0) - J\sum_{m'(\neq m)}(n_{m'\sigma} - n_\sigma^0) \tag{20}$$

(which is dependent on the symmetric Cu 3d orbital m and the σ-spin) is adopted as a spin-polarized state [30]. n^0 and n_σ^0 denote an average occupancy of the 3d orbitals and that of the σ-spin, respectively, and the initial values are taken from the self-consistent LSDA results. U and J are usually orbital dependent in realistic systems. Compared with U, J exerts only a minor influence on the electronic states. It is common to adopt orbital-independent parameters U and J for simplicity [18, 22]. The experimental value of $U = 6.7$ eV [17] and a calculational one of $J = 0.98$ eV [18] for Cu^{2+} in $CaCuO_2$ are used in the following LSDA + U calculation.

$CuGeO_3$ has an orthorhombic structure at room temperature [4, 5] with lattice parameters $a = 4.81$ Å, $b = 8.47$ Å, and $c = 2.94$ Å [10, 11], each unit cell containing two formula units. The crystal structure is characteristic of edge-sharing CuO_6 octahedra, which form $Cu[O(2)]_2$ chains along the c-axis, and where the two apical oxygens and four planar ones are denoted as O(1) and O(2), respectively. In addition, corner-sharing GeO_4 tetrahedra form GeO(1) chains in the same direction [10]. In the following calculations, the numerical atomic basis functions are generated iteratively by solving the H–K–S equation for the isolated atoms in the crystal environment [30], and Cu 3d4s, Ge 4s4p, and O 2s2p orbitals are chosen as the valence states. The Hartree potential is expanded into lattice harmonics up to $\ell_{max} = 4$, and the von Barth–Hedin exchange–correlation potential is adopted. As will be seen below, a consideration of the anisotropic potentials is beneficial to the understanding of the electronic structure for $CuGeO_3$.

3. Results and discussion

The AFM Cu chains deserve more attention due to their leading role in the SP transition of $CuGeO_3$. A doubled cell with AFM ordering along the c-axis contains four formula units. For comparison, the calculation for the NM state is performed first.

The band structure for the NM state is essentially consistent with the previous LAPW result [13], as shown in figure 1. A pair of nearly degenerate half-filled conduction bands with a width of $\sim$1 eV, both composed of d_{xz}, d_{yz}, and O(2) 2p orbitals, appear relatively dispersive along the ΓZ direction parallel to the c-axis but rather flat along other directions perpendicular to the c-axis, indicating a quasi-1D character of the $Cu[O(2)]_2$ chains. Compared with the conduction bands arising from CuO_2 planes with a Cu–O–Cu bond angle of nearly 180° in

both La_2CuO_4 and $YBa_2Cu_3O_7$ [31], however, the present conduction bands are less dispersive due to a strongly bent Cu–O(2)–Cu bond angle [11] of about 99° in $CuGeO_3$. Despite the Cu–O(2) bond length of 1.93 Å [11] being nearly equal to the lengths 1.89 Å for La_2CuO_4 and 1.94 Å for $YBa_2Cu_3O_7$ [31], a strong deformation [11] of $Cu[O(2)]_4$ basal planes in $CuGeO_3$ is considered to reduce the overlap between the Cu 3d and the O 2p orbitals, thus leading to the present narrow band structure. Over a narrow range of energy from -3 to -0.7 eV relative to the Fermi level E_F the occupied d bands are distributed; these are a little mixed with the O 2p bands lying below them. Above E_F, Ge bands appear first—such as both of the lowest unoccupied bands plotted in figure 1. The present result supports the proposal of a strongly ionic character of this compound [17], despite a discernible Ge–O covalent bonding indicated by the Ge–O hybridized states below -7 eV.

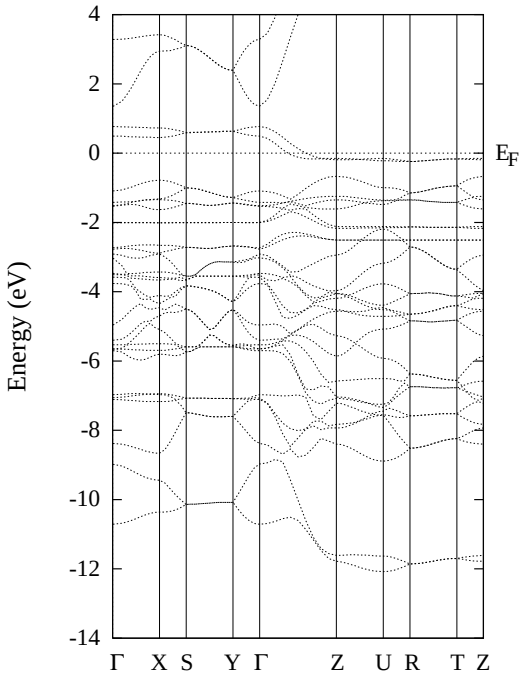

Figure 1. LCAO energy band results for the NM state. The ΓXSYΓ and ZURTZ directions are perpendicular and ΓZ is parallel to the c-axis Cu chain direction. The Fermi level is set as the zero of energy.

The half-filled conduction band structure for $CuGeO_3$ may be unstable with respect to the lattice distortion, as was suggested by the previous result that a supposed dimerization distortion of 0.05 Å opens a gap of about 0.1 eV for this cuprate [13, 14]. The minor gap could be taken as an indication that the lattice distortion favours the formation of the SP phase at low temperature. But one realizes that the gap is too small to account well for the insulating character of this system. It is natural to turn to the investigation of the AFM state.

The present calculation yields an insulating solution for the AFM state with a spin-splitting gap of 0.57 eV, obviously different from the previous metallic result [14] given by the LMTO-ASA calculation. Both of the near-degeneracy conduction bands (see figure 1) split into two pairs of narrow bands, lying on both sides of the Fermi level, as seen in figures 2(a) and 3(a). Primarily distributed above the O 2p bands and with about a 28% mixture of them in the

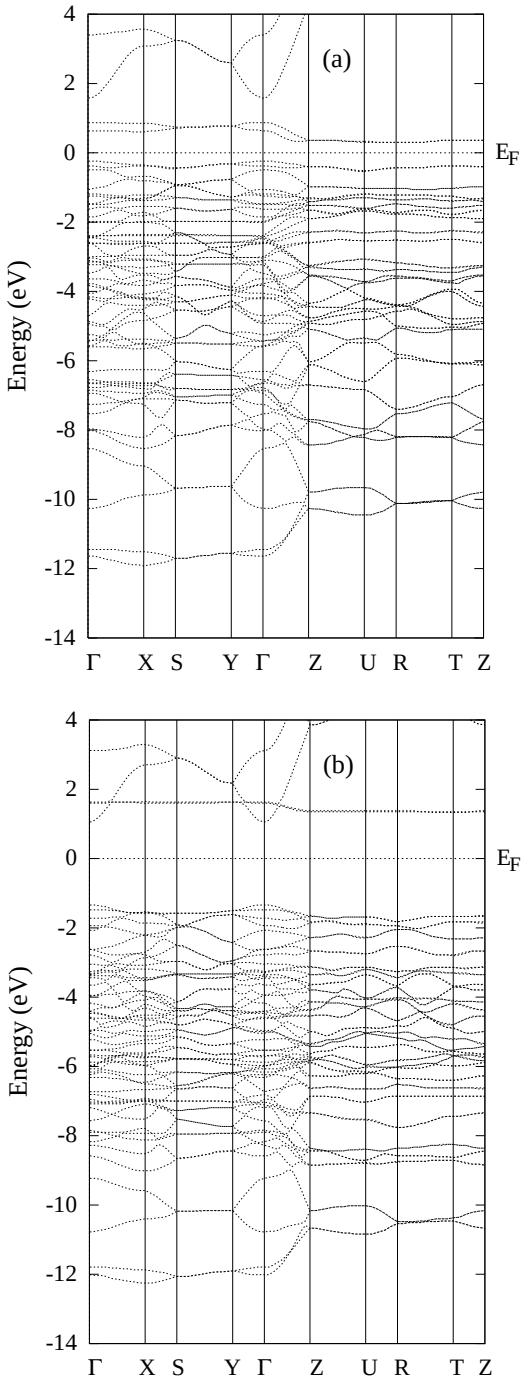

Figure 2. Energy band pictures of the AFM state obtained from (*a*) the LSDA: an insulating gap of 0.57 eV and (*b*) the LSDA + U with $U = 6.7$ eV: a modified band structure and an increased gap of 2.4 eV.

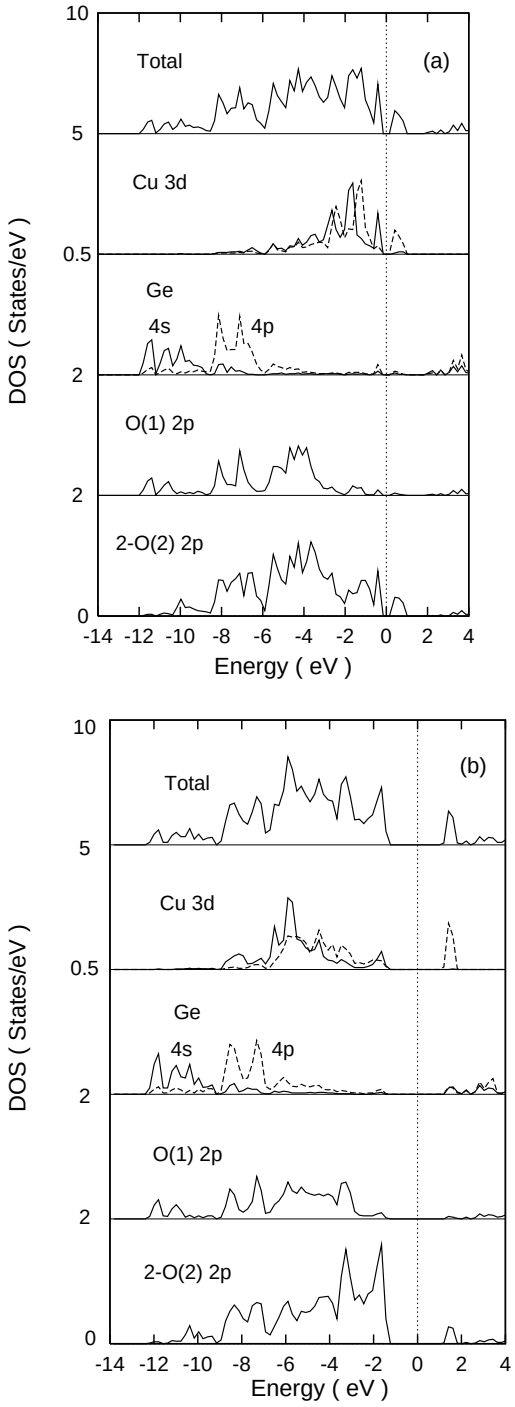

Figure 3. Total and projected densities of states (DOS) per formula unit for the AFM state obtained from (*a*) the LSDA and (*b*) the LSDA + U. For the Cu 3d-projected DOS, the solid (dashed) trace denotes the majority (minority) spin. The vertical dashed line refers to the Fermi level. In (*b*) the 2p–3d CT insulating gap is evident, as well as the enhanced hybridization between the 3d and the 2p states.

topmost valence band, the occupied d bands appear less altered. The unoccupied Ge bands remain almost unchanged. Additionally, a spin moment of 0.46 μ_B per Cu ion is given, 0.3 μ_B carried by the d_{xz} orbital and the rest by the d_{yz} orbital. Such a spin polarization is expected, since both of the orbitals form half-filled conduction bands in the NM state, and naturally they are the most likely ones to 'feel' spin polarized.

The present insulating solution is not surprising. For this case, the charge and spin densities around the Cu ions appear non-spherical due to the non-closed 3d shell and the spin moment, thus leading to the anisotropic Hartree and exchange–correlation potentials, both of which have been treated in the present FP-like calculation. In the LSDA formalism, the exchange potential is dependent on the ratio of the spin density to the total charge density, and the potential is proportional to the ratio if it is a small value, as is the case for solids [31]. Owing to the higher spin density over the d_{xz} and d_{yz} orbitals than over other d orbitals, a stronger exchange potential is seen for the d_{xz} and d_{yz} orbitals than for the other orbitals, thus generating exchange splittings of 0.86 eV for the d_{xz} orbital and 0.63 eV for the d_{yz} one, both larger than that of 0.38 eV for the other orbitals. It is evident that the exchange splittings become orbital dependent due to the anisotropy of the exchange potential. Consequently, the enhanced exchange splittings of the d_{xz} and d_{yz} hybridized bands open the insulating gap of 0.57 eV for this compound. Since the present gap is dominated by the spin splittings, the anisotropic Hartree potential could contribute less, despite the fact that it modifies the energy separation between the spin-like d bands. As stated above, the 3d orbitals become more confined and less hybridized due to the strong deformation of the CuO_4 basal planes. In this sense, the relatively large gap is partly attributed to the narrow band structure of the localized d electrons.

A similar case occurs for the quasi-2D spin-$\frac{1}{2}$ system CaV_4O_9, where, as pointed out by Pickett on the basis of a FP-LAPW calculation, a gap is induced by strongly orbital-dependent exchange splittings: $\sim$1.3 eV for the $d_{x^2-y^2}$ orbital and about 0.4 or 0.6 eV for other unoccupied d orbitals [32]. Additionally, it was shown in his earlier review that an insulating gap is easily opened for La_2CuO_4 due to orbital-dependent spin splittings [31]. Moreover, as indicated by Norman, an orbital polarization leads to a drastic increase of the gap for NiO and accounts for the presence of the insulating gap in FeO, CoO, and La_2CuO_4 [25].

In contrast, when a spherical approximation is adopted for the realistic charge and spin densities, and the potentials, the spherically averaged densities lead to an underestimated exchange potential, thus giving a reduced and orbital-independent exchange splitting. Naturally, the decreasing exchange splitting disfavours the spin-splitting gap and restricts the spin polarization for the d_{xz} and d_{yz} orbitals. Perhaps this is why the previous LMTO-ASA calculation, giving a spin splitting of 0.15 eV and a Cu moment of 0.16 μ_B, yielded a metallic state rather than an insulating one for this compound [14].

It has been seen above that the orbital-dependent exchange splittings induce the insulating solution for this compound, which is an improvement upon the previous metallic one for $CuGeO_3$. However, the present gap is much smaller than the experimental one of about 3.7 eV [16, 17], and it does not exhibit a CT character [16, 17] clearly. This is to be expected for this strongly correlated system, as stated in the introduction. Since the strong-correlation effect of the localized d electrons, implied by the present narrow band structure, has been confirmed by experiment [17], it is worthwhile to carry out the LSDA + U calculation to achieve a better understanding of the insulating property of this material.

The unoccupied d bands shift up and the occupied d bands move down due to the strong on-site Coulomb repulsions, leading to an increased gap of 2.4 eV, as seen in figure 2(*b*). The strong correlation enhances the orbital and spin polarization further, and a subsequent influence appears with the effect that the d_{yz} state is entirely pulled down below E_F and the unoccupied minority-spin d_{xz} bands shift up close to the bottom of the Ge bands. As a consequence, the

Cu 3d orbitals are almost fully filled except the minority-spin d_{xz} orbital with an occupancy of 0.23 e, giving a spin moment of 0.76 μ_B carried entirely by the d_{xz} orbital [23]. Physically, the orbital polarization tends to drive the system towards a full spin polarization, but only a partial polarization is achieved due to the hybridization with the O 2p states [25]. The present spin moment is close to the measured one of 0.7 μ_B [15] reduced by quantum fluctuations [31]. Besides, as shown in figure 3(b), the large downshift of the occupied d bands results in a significant enhancement of the oxygen component at the topmost valence band, which is composed of the O(2) 2p state (about 60%) and the Cu 3d one (nearly 40%), and the lowest unoccupied bands have the d_{xz} character. Compared with the LSDA result above—that the topmost valence band contains an O 2p component amounting to 28%—the present result supports the proposal of a 2p–3d CT insulating character for $CuGeO_3$.

The energy separation between the occupied and the unoccupied d states is of the order of U, as indicated by equation (20). Since a large U usually results in a large gap, it is not surprising that the present gap is smaller than that of 3.02 eV given by the previous LSDA + U calculation with $U = 9.66$ eV, where the unoccupied d_{xz} bands shift up more remarkably and almost lie in the middle of the Ge bands due to the stronger Coulomb repulsions [23]. Additionally, the previous study gave a relatively large moment, namely 0.89 μ_B.

The present band structure is comparable with the x-ray photoelectron valence band spectrum (XPS) [17]. A main and broad structure detected at the binding energy of about 4 eV could be attributed to the emission of the O(2) 2p electrons, according with the CT insulating character and corresponding to a final state d^9L ('L' stands for a ligand hole). The second readily detectable structure at $\approx$8 eV would be assigned to the d^8 state with some contribution from the oxygen states, which is ascribed to an enhanced hybridization between the 3d and the 2p states in the range from -7 to -3 eV relative to E_F, as shown in figure 3(b). Both of the assignments are consistent with the previous ones made on the basis of a comparison between the XPS spectra of $CuGeO_3$ and CuO [17]. In addition, a weak feature at $\approx$16 eV may be related to the emission of the Ge–O(1) electrons from the single-electron states, almost staying at about -11 eV, reflecting the partial Ge–O covalent bonding. But the XPS structure at $\approx$12 eV, which could originate mainly from the d^8 state dominated by the significant correlation effects [17], is not clearly shown in the present calculation. Being a single-particle method in principle, the present approach may be too oversimplified, when considered as a treatment of the genuine many-body interactions, to reproduce all of the details of the experimental XPS spectrum.

The present U-correction improves the LSDA results above remarkably, and gives a satisfactory description for the CT insulating character of $CuGeO_3$, and it also reproduces some main structures of the experimental XPS spectrum. Therefore, it is confirmed that the strong d–d electron correlations play an important role in determining the electronic structure of this compound.

4. Conclusions

The electronic structure calculations have been performed for the spin–Peierls transition system $CuGeO_3$ by using a modified FP-LCAO band method, which is characterized by both an efficient evaluation of multi-centre integrals and a precise treatment of the crystal potential. The LSDA calculation for the AFM state suggests that the strongly orbital-dependent exchange splittings of the narrow Cu 3d bands open an insulating gap of 0.57 eV for the compound. With the on-site Coulomb interaction correction of the localized d electrons, the LSDA + U calculation yields a 2p–3d CT band gap of 2.4 eV and gives a Cu moment of 0.76 μ_B carried by the d_{xz} orbital, both in accordance with the experimental results. In addition, the U-

correction reproduces the main features of the XPS spectrum. In conclusion, the exchange splittings account for a presence of the insulating gap in this cuprate, and the strong d–d electron correlations are responsible for the wide CT gap of this material.

Acknowledgments

One of the authors, H Wu, would like to thank X G Gong, Z Zeng, and L J Zou for their valuable suggestions, and he is grateful to S Y Wang, D Y Sun, and M Z Li for useful discussions. This work was supported by the National Natural Science Foundation of China under the Grant 19574057 and financed by the Grant LWTZ-1289 from the Chinese Academy of Sciences.

References

[1] Hase M, Terasaki I and Uchinokura K 1993 *Phys. Rev. Lett.* **70** 3651
[2] Pouget J P, Regnault L P, Ain M, Hennion B, Renard J P, Veillet P, Dhalenne G and Revcolevschi A 1994 *Phys. Rev. Lett.* **72** 4037
[3] Kamimura O, Terauchi M, Tanaka M, Fujita O and Akimitsu J 1994 *J. Phys. Soc. Japan* **63** 2467
[4] Lorenzo J E, Hirota K, Shirane G, Tranquada J M, Hase M, Uchinokura K, Kojima H, Tanaka I and Shibuya Y 1994 *Phys. Rev.* B **50** 1278
[5] Harris Q J, Feng Q, Birgeneau R J, Hirota K, Kakurai K, Lorenzo J E, Shirane G, Hase M, Uchinokura K, Kojima H, Tanaka I and Shibuya Y 1994 *Phys. Rev.* B **50** 12 606
[6] Zang J, Chakravarty S and Bishop A R 1997 *Phys. Rev.* B **55** R14 705
[7] Riera J and Dobry A 1995 *Phys. Rev.* B **51** 16 098
[8] Castilla G, Chakravarty S and Emery V J 1995 *Phys. Rev. Lett.* **75** 1823
[9] Muthukumar V N, Gros C, Valenti R, Weiden M, Geibel C, Steglich F, Lemmens P, Fischer M and Güntherodt G 1997 *Phys. Rev.* B **55** 5944
[10] Hirota K, Cox D E, Lorenzo J E, Shirane G, Tranquada J M, Hase M, Uchinokura K, Kojima H, Shibuya Y and Tanaka I 1994 *Phys. Rev. Lett.* **73** 736
[11] Braden M, Wilkendorf G, Lorenzana J, Ain M, McIntyre G J, Behruzi M, Heger G, Dhalenne G and Revcolevschi A 1996 *Phys. Rev.* B **54** 1105
[12] Nishi M, Fujita O and Akimitsu J 1994 *Phys. Rev.* B **50** R6508
[13] Mattheiss L F 1994 *Phys. Rev.* B **49** 14 050
[14] Popović Z S, Vukajlović F R and Šlivenčanin Ž V 1995 *J. Phys.: Condens. Matter* **7** 4549
[15] Petrakovski G A, Sablina K A, Vorotynov A M, Kruglik A I, Klimenko A G, Balayev A D and Aplesnin S S 1990 *Zh. Eksp. Teor. Fiz.* **98** 1382 (Engl. Transl. 1990 *Sov. Phys.–JETP* **71** 772)
[16] Bassi M, Camagni P, Rolli R, Samoggia G, Parmigiani F, Dhalenne G and Revcolevschi A 1996 *Phys. Rev.* B **54** R11 030
[17] Parmigiani F, Sangaletti L, Goldoni A, del Pennino U, Kim C, Shen Z-X, Revcolevschi A and Dhalenne G 1997 *Phys. Rev.* B **55** 1459
[18] Anisimov V I, Zaanen J and Andersen O K 1991 *Phys. Rev.* B **44** 943
[19] Czyzyk M T and Sawatzky G A 1994 *Phys. Rev.* B **49** 14 211
[20] Liechtenstein A I, Anisimov V I and Zaanen J 1995 *Phys. Rev.* B **52** R5467
[21] Anisimov V I, Aryasetiawan F and Liechtenstein A I 1997 *J. Phys.: Condens. Matter* **9** 767
[22] Anisimov V I, Korotin M A, Zaanen J and Andersen O K 1992 *Phys. Rev. Lett.* **68** 345
[23] Šlivenčanin Ž V, Popović Z S and Vukajlović F R 1997 *Phys. Rev.* B **56** 4432
[24] Norman M R 1990 *Phys. Rev. Lett.* **64** 1162
[25] Norman M R 1991 *Phys. Rev.* B **44** 1364
[26] Wu H and Zheng Q Q 1998 *J. Phys.: Condens. Matter* submitted
[27] Becke A D 1988 *J. Chem. Phys.* **88** 2547
[28] Delley B 1990 *J. Chem. Phys.* **92** 508
[29] Sobolev S L 1962 *Sibirsk Mat. Zh.* **3** 769
Lebedev V I 1975 *Zh. Vychisl. Mat. Mat. Fiz.* **15** 48
[30] Hugel J and Kamal M 1997 *J. Phys.: Condens. Matter* **9** 647
[31] Pickett W E 1989 *Rev. Mod. Phys.* **61** 433
[32] Pickett W E 1997 *Phys. Rev. Lett.* **79** 1746